# THE LIGHT-SCATTERING MUELLER MATRICES FOR RAYLEIGH AND RAYLEIGH–GANS–DEBYE APPROXIMATION

Jaroslav HOLOUBEK

*Institute of Macromolecular Chemistry, Czechoslovak Academy of Sciences, 162 06 Prague 6*

Received February 12, 1990
Accepted June 11, 1990

Recent theoretical work has shown that the complete set of polarized elastic light-scattering studies should yield information about scatterer structure that has so far hardly been utilized. We present here calculations of angular dependences of light-scattering matrix elements for spheres near the Rayleigh and Rayleigh–Gans–Debye limits. The significance of single matrix elements is documented on examples that show how different matrix elements respond to changes in particle parameters. It appears that in the small-particle limit ($R_g/\lambda < 0{\cdot}1$) we do not loose much information by ignoring "large particle" observables.

The Lorenz–Mie theory[1] which predicts sphere scattering exactly for all size spheres can be approximated with simple models in two regions, where optical and geometrical constants approach a limiting case. One region is the Rayleigh region, where the size of the particle is considered to be very small compared to the wavelength of the scattered radiation. In this case the incident electric field is essentially constant over the entire particle; this approximation permits the small particle to be treated as an electric dipole. The obvious requirement that the external field be considered homogeneous is for spherical particles

$$2\pi R/\lambda \ll 1\,, \qquad (1)$$

where $R$ denotes the sphere radius and $\lambda$ is wavelength in vacuum. However, a second condition is needed for Rayleigh scattering: The size should be small compared with the wavelength inside the particle. Thus, an additional condition is

$$2\pi Rn/\lambda \ll 1\,, \qquad (2)$$

where $n$ is the refractive index of the particle. If only condition (1) is fulfilled, the inner field is not in phase with the external field and we are in the "resonance region". This situation is typical of small conducting particles and does not interest us here.

The other region is the Rayleigh–Gans–Debye region, where the particles can be large, but the refractive index of the particle and that of the surrounding medium are considered to be almost equal. Usually one locates[1] the Rayleigh–Gans–Debye region where the refractive index measured relative to the surrounding medium, $\bar{n}$, is close to 1,

$$a = |\bar{n} - 1| \ll 1 , \tag{3}$$

and the phase shift is small, i.e.,

$$b = 2kR|\bar{n} - 1| \ll 1 , \tag{4}$$

where $k = 2\pi/\lambda$. We will clarify these limiting cases on some examples which show the scattering behaviour of particles with optical parameters on the boundary of this limit.

It is very well known that the properties of light scattered from a particle are related to those of the incident light through a $4 \times 4$ matrix known as the Mueller scattering matrix[1,2] (M matrix). Information about the light scattering properties of the particle or collection of particles is contained in the matrix. Determination of the elements of the matrix, therefore, provides information about the scatterer, which can be related to its optical properties and physical structure. The possibility of a rapid and accurate measurement of the M matrix elements by modulation techniques[3] allows the appropriate matrix elements of a theoretical model to be compared directly with the corresponding experimental values. As a result, light scattering techniques find a wide range of useful applications, which broadens with advances in the experimental determination and theoretical understanding of the M matrix elements. The large number of independent observables[1,2] (10 independent matrix elements for the case of a random suspension of arbitrarily shaped particles) may seem surprising since in the practice of light scattering only one or two polarization ratios at most are usually measured. The traditionally ignored observables may – but need not – provide new structural information.

This paper draws attention to information carried by the individual matrix elements. We discuss the particular form of the M matrix for the Rayleigh particle as a special case of the M matrix for an anisotropic dipolar particle. Furthermore, we compare the corresponding matrix elements for Rayleigh, Rayleigh–Gans–Debye and Lorenz–Mie (LM) particles and shortly comment on the results obtained by an analysis of single matrix elements with the standard approach. Understanding of the entire matrix of a perfect particle (a sphere in our case) provides a basis for gradually improving the matrix when a perfect particle is perturbed into a scatterer irregular in shape or composition.

## THEORETICAL

The basic theory of linear elastic scattering states that the Stokes vector of scattered light, $\mathbf{S}'$, and the Stokes vector of incident light, $\mathbf{S}$, are related by a $4 \times 4$ matrix $\mathbf{M}$, i.e.,

$$\mathbf{S}' = N(n_s k)^4 r^{-2} \mathbf{MS} \tag{5}$$

holds[1,2], where $N$ is the number of scattering particles, $k = 2\pi/\lambda$, $\lambda$ is the wavelength of light, $r$ is the distance from the scattering plane to the detector, and $n_s$ is the refractive index of the surrounding medium. The components of the Stokes vector (usually labelled $\mathbf{I}$, $\mathbf{Q}$, $\mathbf{U}$, and $\mathbf{V}$) are defined in terms of electric field amplitudes parallel ($\mathbf{E}_l$) and perpendicular ($\mathbf{E}_r$) to the scattering plane:

$$\begin{aligned} \mathbf{I} &= \langle \mathbf{E}_l \mathbf{E}_l^* + \mathbf{E}_r \mathbf{E}_r^* \rangle\,, \quad \mathbf{Q} = \langle \mathbf{E}_l \mathbf{E}_l^* - \mathbf{E}_r \mathbf{E}_r^* \rangle\,, \\ \mathbf{U} &= \langle \mathbf{E}_l \mathbf{E}_r^* + \mathbf{E}_r \mathbf{E}_l^* \rangle\,, \quad \mathbf{V} = \mathrm{i} \langle \mathbf{E}_l \mathbf{E}_r^* - \mathbf{E}_r \mathbf{E}_l^* \rangle\,. \end{aligned} \tag{6}$$

The brackets in Eq. (6) denote time averages and the asterisks denote conjugate complex values. The reciprocity theorem[4] states that if the scattering is elastic (equa incident and scattered frequency) and if the sample is macroscopically isotropic the matrix $\mathbf{M}$ assumes a special symmetry given by[4,5]

$$\mathbf{M} = \begin{bmatrix} m_{11} & m_{12} & M_{13} & M_{14} \\ m_{12} & m_{22} & M_{23} & M_{24} \\ -M_{13} & -M_{23} & m_{33} & M_{34} \\ M_{14} & M_{24} & -M_{34} & m_{44} \end{bmatrix}. \tag{7}$$

In a medium fulfilling the assumption of the reciprocity theorem there are ten inde pendent observables. The upper case letters are the "large particle" observables (also called the retardation observables), the lower case letters are the "all-particle" observables (also called the dipole elements), because they do not vanish even in the small particle limit of Rayleigh scatterers. We shall briefly summarize the meaning of some matrix elements in Eq. (7). Element $m_{11}$ is the total scattering power for unpolarized incident light. The well-known Zimm-plot analyses of light scattering are based on the angular and concentrational behaviour of $m_{11}$; in particular, the Rayleigh ratio, $R(\Theta)$, is defined as

$$R(\Theta) = m_{11}(\Theta)/m_{11}(0)\,(1 + \cos^2 \Theta)\,, \tag{8}$$

where $m_{11}(0)$ is $m_{11}$ calculated in the forward direction. Element $m_{12}$ is related to the depolarization ratio measured with vertical and horizontal polarizers. The degree of linear polarization is defined as

$$P = -m_{12}/m_{11} = (i_\perp - i_\parallel)/(i_\perp + i_\parallel)\,, \tag{9}$$

where $i_\perp$ and $i_\parallel$ are the intensities of scattered light at incident linearly polarized light oriented perpendicularly to and in parallel with the scattering plane, respectively. Element $M_{14}$ measures the difference in the scattering power for left and right-circularly polarized incident light and is a measure of particle chirality. It is a parameter important in the circular intensity difference scattering. Elements $M_{14}$, $M_{13}$, $M_{23}$, and $M_{24}$ must vanish if the particle symmetry is such that it exhibits no handedness; accordingly, we often refer to these four elements as to the helicity block. Element $M_{34}$ has a special importance; it is the only element that is never forbidden by symmetry. It may be the only "large-particle" element observable for symmetric particles, i.e., for an LM sphere. The explicit form of the **M** matrix for the LM sphere is given by

$$\mathbf{M}^{\mathrm{LM}} = \begin{bmatrix} m_{11} & m_{12} & 0 & 0 \\ m_{12} & m_{11} & 0 & 0 \\ 0 & 0 & m_{33} & M_{34} \\ 0 & 0 & -M_{34} & m_{33} \end{bmatrix}. \tag{10}$$

The only "large-particle" observables in the sense of Eq. (7) are the $M_{34} = -M_{43}$ elements. Element $m_{22}$ can be used as a measure of the nonspherical shape of scatterers[2]; for scattering spheres the value of $m_{22}/m_{11}$ is unity.

The explicit form of the **M** matrix for a small anisotropic particle characterized by three main components of its polarizability tensor $\alpha_1$, $\alpha_2$, $\alpha_3$ is given[1] by

$$\mathbf{M} = \begin{bmatrix} m_{11} & m_{12} & 0 & 0 \\ m_{12} & m_{22} & 0 & 0 \\ 0 & 0 & m_{33} & 0 \\ 0 & 0 & 0 & m_{44} \end{bmatrix}, \tag{11}$$

where

$$\begin{aligned} m_{11} &= 4A + B - (1/2)(2A + 3B)\sin^2\Theta\,, \\ m_{12} &= (-1/2)(2A + 3B)\sin^2\Theta\,, \\ m_{22} &= (2A + 3B)\left[1 - (1/2)\sin^2\Theta\right], \\ m_{33} &= (2A + 3B)\cos\Theta\,, \\ m_{44} &= 5B\cos\Theta\,, \end{aligned} \tag{12}$$

where

$$\begin{aligned} 15A &= \alpha_1\alpha_1^* + \alpha_2\alpha_2^* + \alpha_3\alpha_3^*\,, \\ 15B &= (1/2)\left(\alpha_1\alpha_2^* + \alpha_2\alpha_3^* + \alpha_3\alpha_1^* + \alpha_2\alpha_1^* + \alpha_3\alpha_2^* + \alpha_1\alpha_3^*\right). \end{aligned} \tag{13}$$

$A$ and $B$ are real quantities; the possibility that the $\alpha$ may be complex is taken into account (asterisks denote conjugate complex values), $\Theta$ is the scattering angle. For an isotropic sphere we have $\alpha_1 = \alpha_2 = \alpha_3 = \alpha$ and it follows from Eqs (*12*) and (*13*) that

$$A = (1/5)\,\alpha^2\,, \quad B = (1/5)\,\alpha^2\,. \tag{14}$$

Substitution of Eq. (*14*) into Eq. (*12*) thus gives after simple rearrangement for the Rayleigh particle

$$m^{\mathrm{R}}_{11} = \alpha^2(1/2)\,(1 + \cos^2\Theta)\,, \quad m^{\mathrm{R}}_{12} = \alpha^2(1/2)\,(\cos^2\Theta - 1)\,, \tag{15}$$
$$m^{\mathrm{R}}_{22} = \alpha^2(1/2)\,(1 + \cos^2\Theta)\,, \quad m^{\mathrm{R}}_{33} = \alpha^2\cos\Theta\,, \quad m^{\mathrm{R}}_{44} = \alpha^2\cos\Theta = m^{\mathrm{R}}_{33}\,.$$

After simple rearrangement this form of the **M** matrix (based on the van de Hulst expression[1]) is exactly equivalent to that used by Bohren and Huffman[2]. Complete information on the intensity and polarization of scattered light is given by Eq. (*5*) with a substitution for **M** from Eqs (*11*) and (*15*). The explicit relation for the Rayheigh particle then is

$$\mathbf{S}' = N(k^4R^6/r^2)\,\beta^2 \begin{bmatrix} (1/2)\,(1+\cos^2\Theta) & (1/2)\,(\cos^2\Theta - 1) & 0 & 0 \\ (1/2)\,(\cos^2\Theta - 1) & (1/2)\,(1+\cos^2\Theta) & 0 & 0 \\ 0 & 0 & \cos\Theta & 0 \\ 0 & 0 & 0 & \cos\Theta \end{bmatrix} \mathbf{S}\,, \tag{16}$$

where $\beta = (n^2 - 1)^2/(n^2 + 2)^2$.

The calculations of $m_{ij}$ are based on the program BHMIE (see ref.[2]). The Rayleigh–Gans–Debye approximation is specified by Eqs (*3*) and (*4*); the corresponding angular dependences are also calculated by means of the MHMIE program.

## RESULTS AND DISCUSSION

The particle parameters used in our calculations are summarized in Table I. The optical parameters of samples 2, 3, and 4 correspond approximately to polystyrene latex spheres in cyclohexane. We investigated the angular dependences of the matrix elements (Eq. (*10*)) for a large LM sphere[1,2] and then forced it into the Rayleigh–Gans–Debye region (Eqs (*3*), (*4*)) by setting the relative refractive index close to unity. We denoted by $m^{\mathrm{R}}_{ij}$ the matrix elements of the Rayleigh particle (Eqs (*1*) and (*2*)). We followed the normalization used in the BHMIE program[2], i.e., $m_{11}$ and $m^{\mathrm{R}}_{11}$ were normalized to 1·0 in the forward direction, the other elements $m_{ij}$ $(i, j \neq 1)$ and $m^{\mathrm{R}}_{ij}$ $(i, j \neq 1)$ were normalized by $m_{11}$ resp. $m^{\mathrm{R}}_{11}$. The angular dependences of $m^{\mathrm{R}}_{ij}$ (Eq. (*16*)) are given in Fig. 1 together with the matrix elements $m_{ij}$ for spheres with growing radius. The matrix elements $m^{\mathrm{R}}_{ij}$ for Rayleigh particles show no oscillation and are either symmetric or antisymmetric about the scattering angle $\Theta = 90°$.

TABLE I

Optical parameters used for calculating the angular dependences of matrix elements $m_{ij}$ (program BHMIE[2]). $R$ is the sphere radius, $n_s$ and $n$ are the respective refractive indices of particle surroundings and of the particle, $R_g$ is the radius of gyration. In the last two columns are the refractive index mismatch (Eq. (3)) and the phase shift (Eq. (4)), respectively, $kR = (2\pi/\lambda)\, R$ is the size parameter

| Sample | $R$, μm | $R_g/\lambda$ | $n_s$ | $n$ | $kR$ | $\lvert\bar{n}-1\rvert$ | $2kR\lvert\bar{n}-1\rvert$ |
|---|---|---|---|---|---|---|---|
| 1 | 1·00 | 1·224 | 1·00 | 1·55 | 9·9292 | 0·55 | 5·73 |
| 2 | 0·0817 | 0·142 | 1·42 | 1·59 | 1·1519 | 0·1197 | 0·1942 |
| 3 | 0·04085 | 0·071 | 1·42 | 1·59 | 0·5760 | 0·1197 | 0·0971 |
| 4 | 0·02042 | 0·035 | 1·42 | 1·59 | 0·2879 | 0·1197 | 0·0485 |

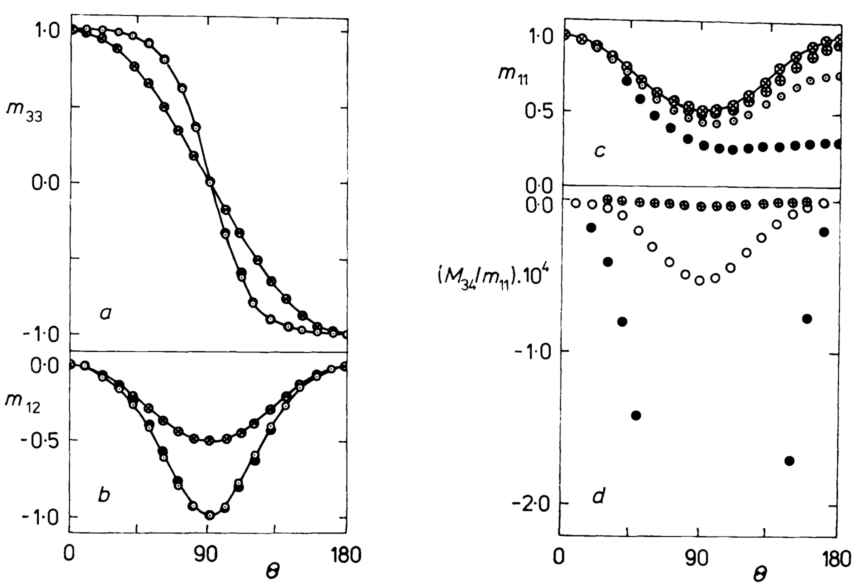


FIG. 1

Angular dependences of matrix elements $m^R_{ij}$ for the Rayleigh particle (Eq. (16)) and of elements $m_{ij}$ for spheres in the Rayleigh–Gans–Debye approximation (Eqs (3), (4)) — samples 2, 3 and 4. The angular plots of $m^R_{12} \cong m_{12}(3) \cong m_{12}(4)$ and $m^R_{33} \cong m_{33}(3) \cong m_{33}(4)$ are indiscernible. *a* $\otimes$ $m^R_{33}$, $\odot$ $m^R_{33}/m^R_{11}$, $\bullet$ $m_{33}(2)/m_{11}(2)$; *b* $\otimes$ $m^R_{12}$, $\odot$ $m^R_{12}/m^R_{11}$, $\bullet$ $m_{12}(2)/m_{11}(2)$; *c* $\otimes$ $m^R_{11}$, $\oplus$ $m_{11}(4)$, $\odot$ $m_{11}(3)$, $\bullet$ $m_{11}(2)$; *d* $\oplus$ $M_{34}(4)/m_{11}(4)$, $\circ$ $M_{34}(3)/m_{11}(3)$, $\bullet$ $M_{34}(2)/m_{11}(2)$

The relationships for $m^R_{ij}$ are independent of particle size, shape and optical properties as long as the particles are much smaller than the wavelength of scattered radiation. The remaining curves in Fig. 1 are the angular dependences of the matrix elements for spheres with radii $R$ increasing from 0·0204 μm to 0·04085 μm and 0·0817 μm. For the smallest sphere ($R$ = 0·0204 μm) the angular dependence of $m_{ij}$ deviates only slightly from the purely symmetric $m^R_{ij}$ curves. The ratios of different matrix elements for angles ranging from 0° to 180° are summarized in Table II for samples 2, 3, and 4. It is interesting that the $M_{34}$ plots show very distinct differences between the compared samples. A comparison of $M_{34}$ column shows that theoretically the $M_{34}$ plots carry much more information than the $m_{11}$ plots. In practice, however, the $M_{34}$ element for small particles is not sufficiently large to be measured reliably as documented in Fig. 2, which shows the absolute maximum of the $M_{34}/m_{11}$ ratio plotted in the double-logarithmic coordinates against $R_g/\lambda$, where $R_g$ is the radius of gyration of a homogeneous sphere; we take $R_g = (3/5)^{1/2} R$. Both $M_{34}$ and $m_{11}$ elements were evaluated at an angle corresponding to the absolute maximum of $M_{34}$. The very steep dependence of $|M_{34}/m_{11}|_{max}$ on $R_g/\lambda$ creates an observability threshold just where the particle departs from the Rayleigh limit, near

TABLE II

Relative angular changes of different matrix elements with increasing sphere size. Comparison between samples 2, 3 and 4 from Table I

| $\Theta$ | $m_{11}(3/2)$ | $m_{12}(3/2)$ | $m_{33}(3/2)$ | $M_{34}(3/2)$ | $m_{11}(4/3)$ | $m_{12}(4/3)$ | $m_{33}(4/3)$ | $M_{34}(4/3)$ |
|---|---|---|---|---|---|---|---|---|
| 0 | 1·000 | — | 1·000 | — | 1·000 | — | 1·000 | — |
| 10 | 1·006 | 1·023 | 1·000 | 0·184 | 1·002 | 1·005 | 1·000 | 0·041 |
| 20 | 1·023 | 1·023 | 1·000 | 0·178 | 1·006 | 1·005 | 1·000 | 0·040 |
| 30 | 1·053 | 1·029 | 0·999 | 0·172 | 1·013 | 1·005 | 0·999 | 0·039 |
| 40 | 1·095 | 1·024 | 0·998 | 0·150 | 1·023 | 1·005 | 0·999 | 0·039 |
| 50 | 1·151 | 1·022 | 0·996 | 0·144 | 1·036 | 1·005 | 0·999 | 0·039 |
| 60 | 1·221 | 1·019 | 0·989 | 0·130 | 1·051 | 1·004 | 0·998 | 0·038 |
| 70 | 1·307 | 1·015 | 0·975 | 0·112 | 1·068 | 1·003 | 0·995 | 0·038 |
| 80 | 1·411 | 1·010 | 0·937 | 0·102 | 1·087 | 1·002 | 0·986 | 0·037 |
| 90 | 1·531 | 1·001 | 0·203 | 0·090 | 1·108 | 1·100 | 0·240 | 0·037 |
| 100 | 1·664 | 0·991 | 1·083 | 0·079 | 1·129 | 0·998 | 1·014 | 0·036 |
| 110 | 1·762 | 0·983 | 1·032 | 0·070 | 1·150 | 1·997 | 1·006 | 0·036 |
| 120 | 1·929 | 0·977 | 1·014 | 0·063 | 1·170 | 0·996 | 1·002 | 0·035 |
| 130 | 2·087 | 0·972 | 1·006 | 0·057 | 1·187 | 0·995 | 1·001 | 0·035 |
| 140 | 2·214 | 0·970 | 1·002 | 0·053 | 1·202 | 0·995 | 1·000 | 0·034 |
| 150 | 2·322 | 0·969 | 1·001 | 0·050 | 1·215 | 0·995 | 1·000 | 0·034 |
| 160 | 2·405 | 0·968 | 1·009 | 0·046 | 1·224 | 0·995 | 1·000 | 0·035 |
| 170 | 2·458 | 0·967 | 1·000 | 0·046 | 1·230 | 0·994 | 1·000 | 0·033 |
| 180 | 2·476 | — | 1·000 | — | 1·231 | — | 1·000 | — |

the radius of one-tenth of the wavelength, as discussed below. The solid line represents our samples 2, 3 and 4, the broken line represents the recent calculations of McClain and Ghoul[6]. As seen in Fig. 2, both calculations give the same slope, the shift of lines is connected with the fact that different refractive indices were used. We can estimate the smallest radius obtainable from Fig. 2 by assuming a specific accuracy of $|M_{34}/m_{11}|_{max}$. If we take $|M_{34}/m_{11}|_{max} = 10^{-3}$, we will not be able to measure $M_{34}$ for particles with $R_g/\lambda$ smaller than about 0·06. Similarly, assuming $|M_{34}/m_{11}|_{max} = 10^{-2}$ we have $R_g/\lambda = 0.13$. We can use the dissymmetry factor[7], $D = m_{11}(45°)/m_{11}(135°)$, for size characterization. The $D$ values for samples 2, 3 and 4 are 2·34, 1·22 and 1·05, respectively. It is very well known that – according to a general rule – the backscattering is somewhat less intensive than the forward scattering for small $kR$. With increasing $kR$ this asymmetry becomes more and more pronounced. Thus, it can be concluded that from the point of view of small particle scattering ($R_g/\lambda < 0·13$) the $M_{34}$ matrix elements (the single non-zero "large-particle" observable for a sphere) do not improve experimental possibilities in comparison with the classical approach of dissymmetry measurement at the present state of detection technique. On the other hand, with increasing size of the sphere this matrix element changes most significantly among all matrix elements. Potential information carried

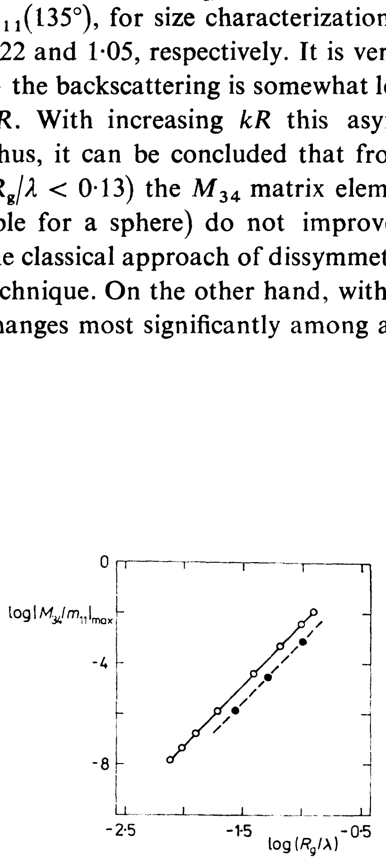


FIG. 2

Dependence of log $|M_{34}/m_{11}|_{max}$ on log $(R_g/\lambda)$. The solid line represents the data of McClain and Ghoul[6], the broken line connects points corresponding to samples 2, 3 and 4. The slope approaches 5 for the plotted size range

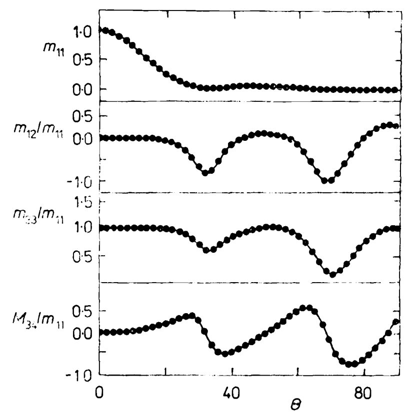


FIG. 3

Angular dependences of matrix elements $m_{11}$, $m_{12}$, $m_{33}$ and $M_{34}$ for the Lorenz–Mie sphere (sample 1, Table I). Note the significant increase of $M_{34}/m_{11}$ element in comparison with Fig. 1. The sign changes are a sensitive measure of the optical parameters of the sphere in this matrix element has been tested by several authors for particles of intermediate diameter (between about a tenth of a wave and a few waves). Examples of angular dependences for sample 1 in this size range are given in Fig. 3. The relative magnitude of the $M_{34}$ element is comparable with other elements. In addition, sensitivity of this element to the optical parameters seems to be higher than that of the $m_{12}$ element (cf. the zero-crossing points for $m_{12}$ and for $M_{34}$). It is noteworthy that the angular dependence of the $M_{34}$ element is very sensitive not only to particle shape (by modelling the particle as a collection of discrete subunits differently distributed in space), but to the refractive indices of the particle and its surrounding[8], and to small structural changes of bioscatterers[9] as well. The role of the $M_{34}$ element is also important when one attempts to characterize irregular particles and their aggregates[10] or in studies of anisotropic particles[11].

## REFERENCES

1. Van de Hulst H. C.: *Light Scattering by Small Particles.* Wiley, London 1957.
2. Bohren C. F., Huffman D. R.: *Absorption and Scattering of Light by Small Particles.* Wiley, New York 1983.
3. Thompson R. C., Bottiger J. R., Fry E. S.: Appl. Opt. *19*, 1323 (1980).
4. Perrin F.: J. Chem. Phys. *10*, 415 (1942).
5. Tian D., McClain W. M.: J. Chem. Phys. *90*, 4783 (1989).
6. McClain W. M., Ghoul W. A.: Biopolymers *26*, 2027 (1987).
7. Heller W., Nakagaki M.: J. Chem. Phys. *31*, 1188 (1959).
8. Bickel W. S., Watkins A. J., Videen G.: Am. J. Phys. *55*, 559 (1987).
9. Bickel W. S., Stafford M. E. in: *Light Scattering by Irregularly Shaped Particles* (D. W. Schuerman, Ed.), p. 299. Plenum Press, New York 1980.
10. Bottiger J. R., Fry E. S., Thompson R. C. in: *Light Scattering by Irregularly Shaped Particles* (D. W. Schuerman, Ed.), p. 283. Plenum Press, New York 1980.
11. Holoubek J.: J. Polym. Sci. B, submitted.

Translation revised by M. Kubín.